



Original Article

Corresponding Author

Zan Chen

<https://orcid.org/0000-0002-0104-115X>

Department of Neurosurgery, Xuanwu Hospital, Capital Medical University, No. 45, Changchun Street, Xicheng District, Beijing 100053, China
Email: chenzan66@163.com

Received: September 8, 2021

Revised: December 21, 2021

Accepted: December 28, 2021

*Qiang Jian and Zhenlei Liu contributed equally to this study as co-first authors.



This is an Open Access article distributed under the terms of the Creative Commons Attribution Non-Commercial License (<https://creativecommons.org/licenses/by-nc/4.0/>) which permits unrestricted non-commercial use, distribution, and reproduction in any medium, provided the original work is properly cited.

Copyright © 2022 by the Korean Spinal Neurosurgery Society

INTRODUCTION

The cervical lateral mass is composed of a superior and inferior zygapophysis of the same segment and the isthmus between them. The superior and inferior facets and capsule of the 2 adjacent segments constitute the facet joints of the cervical spine. In Louis's 3-column spine concept, bilateral facet joints have an important role in axial stability structure, which consists of 2 columns (bilateral facet joints) at the C1–2 level and 3 columns (the anterior vertebral bodies and discs, together with the 2 posterior facet joints) from C2 to the sacrum.¹ Bilateral facet joints, together with the anterior vertebral body and intervertebral disc, form the intervertebral connection and maintain structural stability of the cervical spine.²

Cervical spine damage and loss of stability may be due to tumor, infection, trauma, or surgery. In particular, posterior sur-

Reconstruction of the Cervical Lateral Mass Using 3-Dimensional-Printed Prostheses

Qiang Jian*, Zhenlei Liu*, Wanru Duan, Jian Guan, Fengzeng Jian, Zan Chen

Department of Neurosurgery, Xuanwu Hospital, Capital Medical University, Beijing, China

Objective: This study aimed to investigate the outcome of using 3-dimensional (3D)-printed prostheses to reconstruct a cervical lateral mass to maintain cervical stability.

Methods: We retrospectively analyzed data of 7 patients who underwent cervical lateral mass reconstruction using a 3D-printed prosthesis, comprising axial and subaxial lateral mass reconstruction in 2 and 5 patients, respectively. Bilateral mass was reconstructed in 1 patient and unilateral mass in the remaining 6 patients.

Results: Using a 3D-printed lateral mass prosthesis, internal fixation was stable for all 7 patients postoperatively. No implant-related complications such as prosthesis loosening, displacement, and compression were observed at the last follow-up.

Conclusion: Reconstruction of the lateral mass structure is beneficial in restoring load transfer in the cervical spine under physiological conditions. A 3D-printed prosthesis can be considered a good option for reconstruction of the lateral mass as fusion was achieved, with no subsequent complications observed.

Keywords: Lateral mass, Prosthesis, Three-dimensional printing, Axis, Subaxial cervical spine

gery for cervical vertebral tumors or dumbbell tumors often involves total or partial resection of the lateral mass, resulting in a loss of the cervical spine's load-bearing structure.³ At present, a screw rod system is commonly used for internal fixation to maintain cervical spine stability. However, reconstruction of the lateral mass structure has rarely been reported.

Three-dimensional (3D)-printing, an additive manufacturing method, is a process in which 3D models are created through successive layers based on a computer-aided design.⁴ It is widely used in the field of spinal surgery due to its favorable mechanical strength, capacity to manufacture highly individualized shapes, potent osteoinductivity, and osseointegration.⁵⁻¹⁰ At our center, upper and subaxial cervical lateral masses were reconstructed using 3D-printed prostheses for 7 patients with cervical tumors. In this study, clinical data were retrospectively analyzed and relevant studies concerning lateral mass reconstruction were re-

viewed. To our knowledge, this is the first study on reconstruction of cervical lateral mass using 3D-printed prostheses.

MATERIALS AND METHODS

1. Study Design

Clinical data of patients who had undergone an implant using a 3D-printed lateral mass prosthesis for reconstruction of the cervical lateral mass structure at Department of Neurosurgery, Xuanwu Hospital were retrospectively analyzed. Due to its retrospective design, the requirement of written informed consent was waived.

2. Clinical Data

From December 2018 to January 2021, 7 patients received a lateral mass prosthetic implant at Department of Neurosurgery, Xuanwu Hospital, including 2 patients with axial tumors and 5 patients with dumbbell tumors of the subaxial cervical spine, one of whom had vertebral body involvement. Unilateral prosthesis was implanted in 6 patients and bilateral prostheses in 1 patient.

Prior to the first operation, all patients had undergone preoperative plain radiographic, computed tomography (CT), and magnetic resonance imaging (MRI) examinations. For patients with vertebral tumors, a preoperative puncture biopsy was performed to determine the nature of the vertebral tumor. Based on preoperative imaging data evaluation, the range of bone structures to be excised (lateral mass resection or total *en bloc* spondylectomy) was considered prior to designing the corresponding lateral mass and the anterior column prosthesis.

3. Prosthesis Design

1) Data and software

Patients' CT data were obtained, and Mimics software (ver. 21.0, Materialize HQ Technologielaan, Leuven, Belgium) was used for modeling to generate *Standard Triangle Language* files, which were then imported into 3-matic software (ver. 13.0, Materialize HQ Technologielaan) for prosthesis design.¹¹

2) Axial anterior column prosthesis

The prosthesis was designed to be in direct contact with both the endplate of the C3 vertebral body and the articular surface of the inferior facet of C1. The superior bilateral articular surface of the axial anterior column was designed to occupy the anterior two-thirds of the articular surface of the inferior facet of the atlas. The prosthesis was designed to form a self-stabiliz-

ing structure through fixing 4 screws to the superior and inferior vertebral bodies. Two screws fixed to C1 were tilted backward and upward to fix onto the lateral mass of the atlas, and 2 screws fixed to C3 were tilted backward and downward to fix onto C3's vertebral body.

3) Axial lateral mass prosthesis

The superior facet articular surface of the axial prosthesis was designed to occupy the posterior one-third of the atlas's inferior facet articular surface, and the inferior facet articular surface of the prosthesis was matched to the C3 superior zygapophysis. The screw attached to C3 was tilted inward and attached to the C3 lateral mass.

In the early stage, we expected to achieve a more stable prosthetic combination with fewer fixed levels. Therefore, bilateral screw trajectories were designed for the body part of the anterior column and lateral mass prosthesis, with the expectation of achieving a 3-column stable structure through fixing the anterior column and bilateral lateral mass prostheses together using 2 anterior screws.

At a later stage, the lateral mass prosthesis was designed to form a self-stabilizing structure with 2 screws attached to the adjacent lateral masses without a common screw trajectory on the body part of both anterior column and lateral mass prosthesis.

4) Subaxial cervical lateral mass prosthesis

A subaxial cervical lateral mass prosthesis directly matched the facet articular surface of the adjacent lateral masses, thus avoiding invasion of the vertebral artery. The prosthesis was fixed with 2 screws to form a self-stable structure. The pedicle screws fixed to C2 and T1 were inclined inward, with the remainder being lateral mass screws.

5) Print material and hardware

Prostheses were made using a porous structure consisting of regular dodecahedral units (porosity range, 60%–80%; pore size range, 400–600 μm). The 3D data file of the designed prosthesis was printed by ARCAM EBM Q10 printer, and the printing powder used was Ti6Al4VELL, in accordance with the ASTM F300L standard. Postprocessing, the printed prosthesis was placed into the patient and fixed.¹¹

4. Research Parameters

Patients' imaging and clinical effect data were retrospectively analyzed. Imaging data included tumor location, postoperative

recurrence, and prosthesis stability. An absence of instrumentation failure or loosening and subsidence of the caudal end of the lateral mass prosthesis was considered evidence of fusion. Clinical effects were evaluated using the 17-point scoring system of the Japanese Orthopedic Association (JOA).

5. Follow-up

CT 3D reconstruction and MRI scans were reexamined prior to discharge and postoperatively at 3, 6, and 12 months. JOA scores and complications were recorded at the last follow-up.

RESULTS

Demographic data concerning the 7 study patients are summarized in Table 1. The average age of the patients was 47 years (range, 16–73 years). Three patients had chordomas, 2 of which were primary chordomas of the axial vertebrae. Two patients had schwannomas and 1 patient had a metastatic tumor. Four patients had subaxial cervical spine involvement and presented with dumbbell-shaped tumors. All patients had undergone intralesional excisions. The mean follow-up time was 10 months (range, 3–32 months). Patients’ symptoms had improved significantly at follow-up. Tumor recurrence occurred in one patient. All patients had undergone internal fixation and none of the implants had failed.

1. Illustrative cases

1) Case number 1

A 63-year-old man was admitted to our hospital with right shoulder pain. Preoperative CT and MRI scans showed an axial tumor (Fig. 1A, B). The tumor was staged as IIB, according to the Enneking system,¹² and as Weinstein-Boriani-Biagini 5–10, A–D, according to the Weinstein-Boriani-Biagini classification.¹³ The tumor was confirmed to be a chordoma on transoral puncture biopsy.

Posterior cervical surgery was first performed to completely remove the posterior column structure of the axis, including the spinous process, lamina, inferior articular process and posterior wall of the axial transverse process foramen, to expose and dissociate the bilateral V3 segment of the vertebral arteries and C3 nerve roots, remove the anterior axis transverse process nodules in front of the vertebral artery, and remove the posterior 1/3 of the superior axis articular process above the V3 segment of the bilateral vertebral arteries. Finally, bilateral axial lateral mass prostheses were placed and fixed using a posterior screw rod system (Fig. 1C, D).

Table 1. Seven patients with lateral mass reconstruction

Case No.	Age (yr)/sex	Lesion	Lateral mass span	Reconstruction material	Clinical manifestation	Preoperative JOA score	Follow-up (mo)	Adjuvant therapy	Complication	JOA score at final follow-up
1	63/M	C2 chordoma	Bilateral C2	3D-printed titanium alloy prosthesis	Neck pain, shoulder pain, dysphagia	15	32	Radiation therapy	Dysphagia after radiotherapy	17
2	73/M	C2 chordoma	Right C2*	3D-printed titanium alloy prosthesis	Neck pain, dysphagia	15	9	None	None	17
3	16/M	C6-7 chordoma	Right C6-7	3D-printed titanium alloy prosthesis	Upper limb pain	14	14	None	Recurrence	16
4	62/F	C6-7 metastasis	Left C6-7	3D-printed titanium alloy prosthesis	Upper limb pain and weakness	15	5	Chemo-therapy	None	16
5	49/M	C3/4 dumbbell schwannoma	Right C3-4	3D-printed titanium alloy prosthesis	Upper limb numbness	16	6	None	None	17
6	28/M	C6-7 dumbbell schwannoma	Right C6-7	3D-printed titanium alloy prosthesis	Upper limb pain	15	4	None	None	17
7	42/F	C6-7 schwannoma	Left C6-7	3D-printed titanium alloy prosthesis	Limb numbness	14	3	None	None	16

JOA, Japanese Orthopedic Association; 3D, 3-dimensional.

*Matching error.

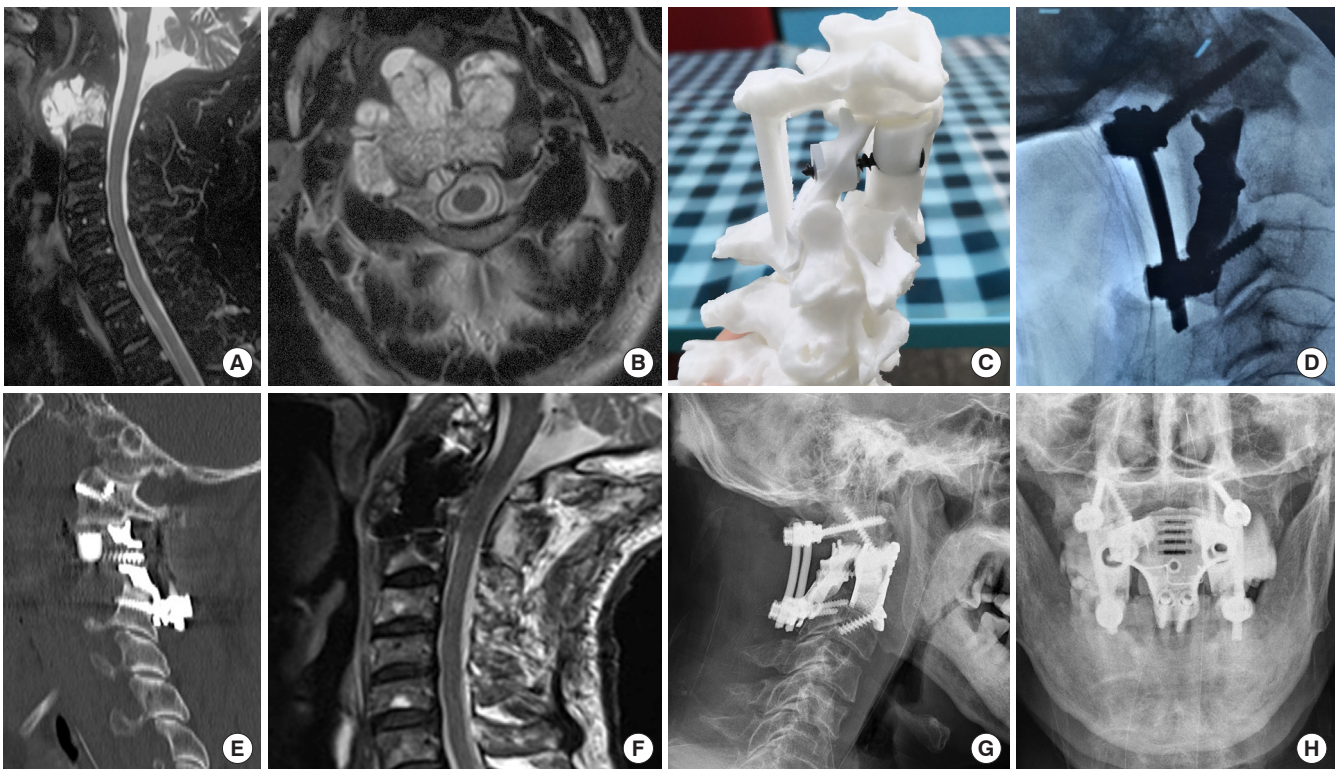


Fig. 1. Imaging findings for case number 1. Sagittal contrast-enhanced magnetic resonance imaging (MRI) (A) and axial T2-weighted MRI (B) showing an axial tumor (Enneking stage IIB). The Weinstein-Boriani-Biagini stages were 5–10, A–D. Preoperative puncture pathology indicated chordoma. (C) A preoperative design of the 3-dimensional-printed axial lateral mass (LM) prosthesis. (D) An intraoperative image shows the implantation of the posterior LM prosthesis. (E) A postoperative sagittal computed tomography scan of the reconstruction shows that the LM prosthesis is in a good position and that the anterior screw was inserted into the anterior column and LM prostheses. (F) Postoperative sagittal T2-weighted MRI indicates good spinal canal volume. Postoperative lateral (G) and anteroposterior (H) radiographs of the cervical spine show that the LM prosthesis is well positioned.

After complete disinfection of the oral and nasal cavities with iodophor, in a supine position, the patient's mouth was opened with a mouth opener, and the mucosa and muscle of the posterior pharyngeal wall were cut open. The tumor was visible on the axial surface, and part of the tumor was removed to fully expose the anatomical structure. The anterior atlas arch and axial odontoid process were removed, the C2/3 disc was removed, then the axial vertebral body was resected with the tumor. The dural sac was explored, and the tumor on the dural surface was completely removed. A 3D-printed axial prosthesis was placed, the lateral mass of the atlas was fixed cephalally with screws, and the upper margin of the C3 vertebral body was fixed caudally with screws. The anterior column prosthesis and the posterior lateral mass prostheses were fixed with a single screw, as the shared trajectory of the screw secured the 3-column fixed structure. The muscles and mucosa of the larynx wall were sutured in layers, and a nasal feeding tube was placed.

Wound healing of the posterior pharyngeal wall was determined using television fibrolaryngoscopy on day 7 postoperatively. Wound healing was satisfactory. The gastric tube was removed and a fluid diet was provided. Postoperative imaging showed a satisfactory match (Fig. 1E–H). After discharge, the patient received proton beam radiation therapy for residual disease and developed dysphagia after radiotherapy, without any other discomfort; the patient declined further imaging examination in the follow-up.

2) Case number 3

A 15-year-old male patient presented to our hospital with neck and upper limb pain and weakness in both lower limbs. Physical examination showed 4+ muscle strength grading of both lower extremities and knee reflex grading +++. MRI showed right C5/6 and C6/7 dumbbell-shaped tumors, involving C6–7 vertebral bodies (Fig. 2A, B). CT angiography revealed occlu-

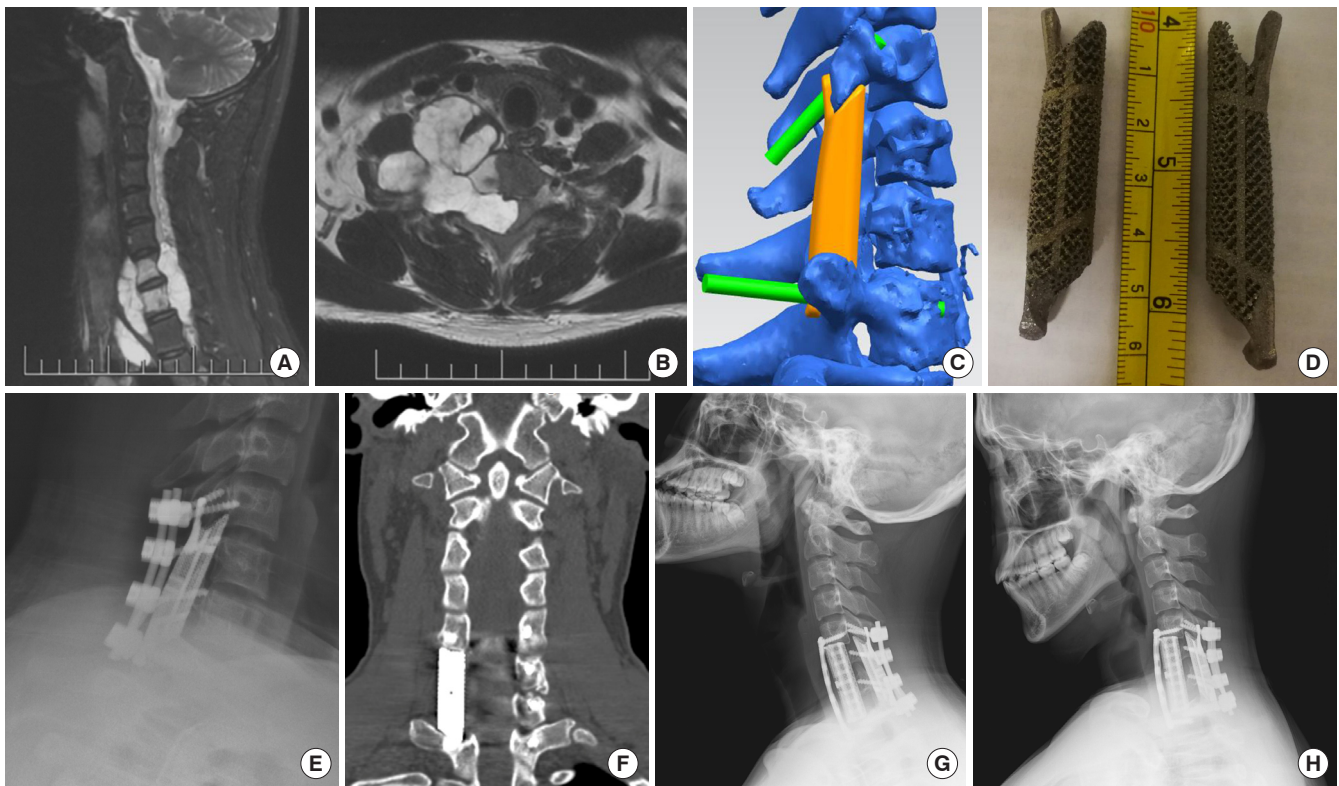


Fig. 2. Imaging findings for case number 3. (A, B) Preoperative contrast-enhanced sagittal and axial T2-weighted magnetic resonance imaging shows a dumbbell tumor with C6/7 vertebral body involvement. Preoperative biopsy pathology indicated chordoma. (C) The lateral mass (LM) prosthesis was preoperatively designed based on the patient's computed tomography (CT) data, and (D) the 3D-printed LM prosthesis was manufactured. (E) The first-stage posterior approach was used to remove the intraspinal tumor and reconstruct the LM structure. (F) A coronal CT scan of the reconstruction at 6 postoperative months shows that the LM prosthesis is in a good position. Dynamic radiographs taken in extension (G) and flexion (H) showed the stability of the implant.

sion of the right vertebral artery. Preoperative puncture pathology showed a false-negative result. The tumor was removed, and cervical spine stability was reconstructed in 2 stages after tumor arterial embolism.

In the first stage, resection of the intraspinal tumor and reconstruction of the lateral mass were performed via the posterior approach. We removed the cervical 6/7 spinous process, and the right semilamina and lateral masses to expose the epidural tumor invading along the foramina. The tumor had destroyed the transverse process and pedicle, and there was an abundant blood supply surrounding the vertebral artery. Intralaminar excision of the intraspinal and partial paravertebral tumors was performed under microscopy. The right spinal nerves of C7–8 appeared to be well protected. An intraoperative rapid frozen section revealed a chordoma. A 3D-printed lateral mass prosthesis was implanted on the right side (Fig. 2C–E).

Seven days later, a secondary anterior paravertebral and ver-

tebral tumor resection and an anterior column prosthesis reconstruction were performed. An anterior oblique incision was made to expose the anterior vertebral body. The tumor was visible on the spine surface. After part of the tumor was removed, C-arm x-ray fluoroscopy was used to determine the C5/6 and C6/7 intervertebral disc and related vertebral bodies. After the intervertebral discs and posterior longitudinal ligament were resected, the tumor together with the C6 and C7 vertebral bodies were then removed. An anterior vertebral body prosthesis of an appropriate size was placed between C5 and T1, and an anterior titanium plate was fixed with 4 screws. The internal fixation position of the C-arm was confirmed to be satisfactory, and a drainage tube was placed paraspinally.

The drainage tube was removed on postoperative day 1. Post-discharge, the patient did not receive proton beam radiation. Six-month follow-up imaging examinations indicated that the implant was in a good position (Fig. 2F–H). However, the tu-

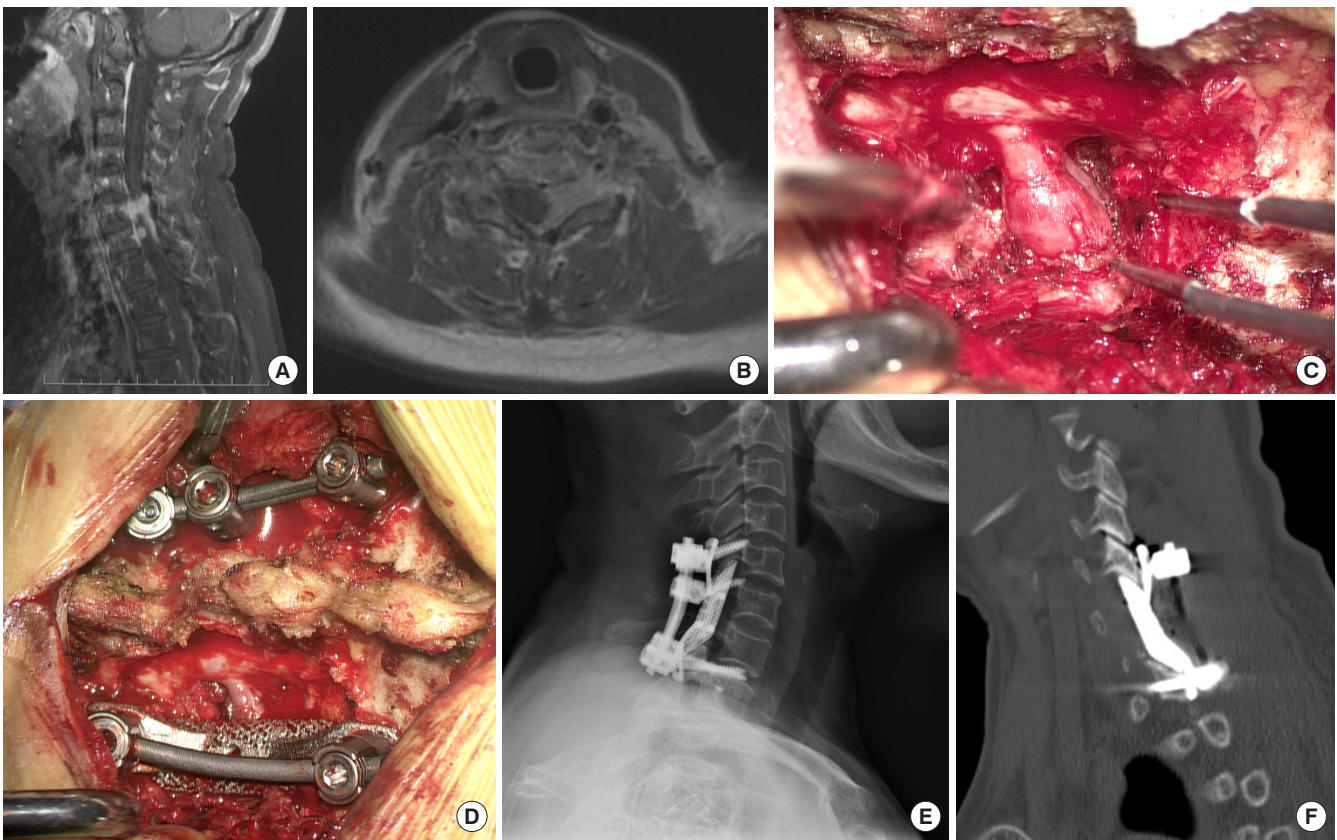


Fig. 3. Imaging findings for case number 4. Enhanced sagittal (A) and axial T2-weighted (B) magnetic resonance imaging findings indicate left dumbbell tumors at C6/7 and C7/T1. (C) Tumor infiltration of the nerve root was observed intraoperatively, and (D) a lateral mass prosthesis was implanted following tumor resection. Postoperative lateral cervical radiograph (E) and sagittal computed tomography scan images of the reconstruction (F) show that the prosthesis was well positioned and that it was highly matched with the surrounding structures.

mor recurred at a later date.

3) Case number 4

A 62-year-old woman presented with pain and weakness in her left arm. MRI revealed a left C5–7 dumbbell-shaped tumor (Fig. 3A, B). Ultrasonography findings concerning the brachial plexus indicated left C7 thickening (left, 42 mm²; right, 18 mm²) compared with that on the contralateral side, decreased echo of the nerve bundle, and enhanced echo of the perineurium. Due to a previous history of breast cancer, metastatic cancer was highly suspected.

A posterior cervical approach was undertaken to expose the bilateral C5/T1 lamina and to excise the left lamina, the lateral mass, and the C6/7 pedicle. The tumor was attached to the dural surface and spinal nerve roots were involved. After resection, the spinal nerve root was swollen (Fig. 3C). A 3D-printed prosthesis was placed and fixed with a T1 pedicle screw and a C5 lateral mass screw (Fig. 3D).

Postoperatively, this patient reported no further pain in the left arm, and radiographic examinations taken prior to discharge showed that the prosthesis remained in a good position (Fig. 3E, F).

DISCUSSION

In spinal cord tumors, the incidence rate of spinal dumbbell tumors is reported to be approximately 18%, and is mainly located in the cervical segment.¹⁴ Although total *en bloc* spondylectomy is not required, the lateral mass should be removed to expose the tumors in the intervertebral foramen. Internal fixation is needed to stabilize the cervical spine when >50% of the facet joint is removed,¹⁵ but few studies have reported reconstruction of the lateral mass structure of the cervical spine (Table 2).^{16–28} For primary cervical vertebral tumors, reconstruction of spinal stability after spondylectomy is challenging. Most studies have reported reconstructing the vertebral structure of the

Table 2. Literature review concerning lateral mass reconstruction

Study	Age (yr)/sex	Pathology	Lateral mass span	Reconstruction material
Bongioanni et al., ¹⁶ 1996	36/M	Aneurysmal bone cyst	C1	An iliac-crest bone graft
Suchomel et al., ¹⁷ 2007	62/M	Chordoma	Bilateral C2	Harms mesh cage
Wang et al., ¹⁸ 2009	12/F	Aneurysmal bone cyst	Bilateral C1	Titanium mesh cage, rib graft
Chung et al., ¹⁹ 2012	48/M	Osteosarcoma	C1	Titanium mesh cage
Jandial et al., ²⁰ 2013	27/M	Metastatic Ewing sarcoma	Bilateral C1	Expandable cages
Winking, ²¹ 2014	54/F	Nodular plasmocytoma	C1	Harms cage
Bobinski et al., ²² 2015	48/F	Angiosarcoma	C1	2 Titanium cages
	54/M	Multiple myeloma	C1	Titanium cage
Clarke et al., ²³ 2015	35/M	Chordoma	Oc–C3	Titanium mesh cage
	60/F	Chondrosarcoma	C1–6	Titanium mesh cage
	50/M	Epithelioid schwannoma	Oc–C3	Titanium mesh cage
	61/F	Dumbbell schwannoma	C3–5	Titanium mesh cage
	77/F	Chordoma	Left, Oc–C4; Right, Oc–C3	Titanium mesh cage
	16/M	Schwannoma	C6–T1	Fibular strut
	25/M	Osteochondroma	C3–6	Fibular strut
Clarke et al., ²⁴ 2016	8/F	Osteosarcoma	Bilateral C1	Allograft fibular strut
Peciu-Florianu et al., ²⁵ 2017	12/M	Osteoblastoma	Bilateral C1	Titanium cages
Stephens and Wright, ²⁶ 2017	27/M	Eosinophilic granuloma	C1	A titanium expandable cage
Neva et al., ²⁷ 2017	18/F	Aneurysmal bone cyst	C1	Static titanium cage
Ji et al., ²⁸ 2020	50/F	Schwannoma	C3–4	A strip of shaped allograft bone

anterior column only in conjunction with the posterior screw rod internal fixation system to maintain cervical spine stability.^{29,30}

Each vertebra of the upper cervical spine has particular morphological and biomechanical characteristics. The bilateral lateral mass of the atlas bears the entire weight of the head and, for this reason, reconstruction of the lateral mass structure is more common in cases of atlas lesions than in cases of axial lesions. Furthermore, the axial vertebra plays a unique role in the distribution of axial loads, transferring the weight carried through the bilateral superior facets to the 3 columns, namely, the anterior vertebral body and bilateral lateral mass joints.³¹ We defined the lateral mass of the axis as a columnar structure connecting the facet from C1 to C3. Reconstruction of the lateral mass of the axial vertebra has rarely been reported, and reconstruction of the vertebral body of the anterior column appears to be the most common type involved. Stulik et al.³² reported reconstruction of the C2 anterior column using a titanium cage connecting the anterior arch of the atlas or the basilar clivus to the C3 superior endplate. Ames et al.³³ reported 3 successful cases of reconstruction of the C2 anterior column using Steinmann pins and methylmethacrylate. Jeszenszky et al.³¹ de-

signed a C2 anterior column prosthesis through studying axial morphology. Xu et al.⁶ and Hunn et al.³⁴ reconstructed the C2 anterior column vertebral body using 3D-printing technology. A common feature of all of these studies is the transfer of the axial load from bilateral columns of C1 lateral masses to the C3 anterior column, assisted using posterior fixation. In contrast to these studies, Suchomel et al.¹⁷ reconstructed the axial's 3-column structure. Bilateral axial lateral masses were reconstructed using titanium cages; however, the anterior column structure of the titanium cage directly connected the basilar clivus to the C3 vertebral body. While these studies reported successful reconstructions and integration, the reconstructions did not conform to the normal axial load transmission of the human body. The characteristics of the 3D-printed axial lateral masses designed in this study involved the articular surface area of the axis superior facet occupying one-third of the total inferior facet of the atlas, and the inferior facet directly connecting to the superior facet of C3. In combination with the anterior column prosthesis, the load carried through the bilateral C1 lateral masses was transferred to the anterior C3 vertebral body and the bilateral lateral mass joints to reconstruct the normal C2 structure and restore the normal two-column load bearing and 3-column load

distribution.

The vertebrae of the subaxial cervical spine are ordinary and morphologically similar to one another. Unlike the facet joints of the lumbar spine, the posterior subaxial cervical facet carries 64% of the cervical axial load.³⁵ Various studies have reported a variety of strategies for reconstruction of the subaxial lateral mass. Ji et al.²⁸ reported a case of C3–4 lateral mass reconstruction using an allograft, and they performed a biomechanical evaluation of a cadaver specimen for the reconstruction of the subaxial lateral mass. Clarke et al.²³ reported 7 cases of subaxial lateral mass reconstruction using either titanium cages or ribs. However, more implants can increase risks during and after surgery. In the largest sample size series reported by Clarke et al.²³ (7 cases of lateral mass reconstruction), implant fixation system failure occurred in 2 patients. We consider that the reconstruction material (titanium cage) was an important reason for its failure. The titanium cage needs to be pruned intraoperatively and fitted over the articular process of adjacent segments. It is difficult to prune the titanium cage to an appropriate size by hand. Moreover, its use increases the risk of compression of the vertebral artery. Furthermore, the titanium cage has a cylindrical structure, which does not take the physiological curvature of the cervical spine into account. Thus, the application of a titanium cage cannot correct the physiological curvature of the cervical spine.

For resolving such challenges, 3D printing is a promising solution. The advantages of individualized 3D-printed prostheses are as follows. First, the design of the 3D-printed prosthesis is flexible and more individualized. These prostheses can completely reconstruct the multi-column mechanical support structure of the upper and subaxial cervical spine, in a manner that conforms more closely to the biomechanical characteristics of the normal human body, which theoretically avoid the shift in load above the bone defect to the screw and rod system. In addition, for cases involving a combined approach, the shared screw trajectory of the anterior column and lateral mass prosthesis can also be designed. These devices further improve the immediate stability of the prosthesis. Second, through the use of computer-aided design, 3D-printed prostheses possess high accuracy to precisely match the bone structure.³⁶ Compared with traditional structural reconstruction (titanium cage or fibular strut), there is no need for intraoperative trim or fibular graft, which reduces the difficulty of surgery and reduces operating time.^{11,37} To better match the 3D-printed lateral mass prosthesis, we designed the lateral mass prostheses of different heights which facilitate the contact with the cephalic and caudal cervi-

cal structures and enable axial load bearing for some patients. In our patient group, the 3D-printed prosthesis was well matched during the operation, with prosthesis fitting error occurring in only one patient. Third, the microporous structure of the 3D-printed prosthesis has an appropriate pore size and porosity to achieve long-term stability of the spine through osteoinductivity, and osseointegration.^{5–11} Compared with polyetheretherketone (PEEK) or plasma sprayed porous titanium-coated PEEK, a 3D-printed porous titanium prosthesis possesses stronger biomechanical stability, mechanical strength, and better osseointegration.³⁸ Through reconstructing the lateral mass prosthesis, which acts as an interarticular bone graft bed, the graft space and bone conduction of the lateral mass structure of the cervical spine can be increased. However, 3D-printing technology has the following disadvantages. First, if more structures are removed intraoperatively, a prosthesis fitting error may occur, so it is necessary to carefully review the imaging data prior to surgery to determine the resection range and accordingly design the shape and size of the prosthesis. In this patient group, 1 patient had a prosthesis fitting error due to excessive intraoperative resection. Second, as 3D-printing technology is costly, the economic burden on patients is an issue. Third, the prosthesis has no locking device; hence, a posterior titanium rod and an anterior titanium plate were added in some patients to lock the screws. Thus, the long-term effects of screw loosening require further follow-up.

This study was limited in that there was an absence of biomechanical evaluations and a numeric value concerning axial load sharing was not determined. Future research is required to verify this understanding of load sharing using finite element analysis.

CONCLUSION

Reconstruction of the lateral mass structure is beneficial for restoring load transfer in the cervical spine under physiological conditions. A 3D-printed prosthesis is a good choice for reconstruction of the lateral mass to achieve fusion.

NOTES

Conflict of Interest: The authors have nothing to disclose.

Funding/Support: This study received no specific grant from any funding agency in the public, commercial, or not-for-profit sectors.

Author Contribution: Conceptualization: ZC; Data curation:

QJ, WD, JG; Writing - original draft: QJ; Writing - review & editing: Zu, FJ.

REFERENCES

- Louis R. Spinal stability as defined by the three-column spine concept. *Anat Clin* 1985;7:33-42.
- Izzo R, Guarnieri G, Guglielmi G, et al. Biomechanics of the spine. Part I: spinal stability. *Eur J Radiol* 2013;82:118-26.
- Asazuma T, Toyama Y, Maruiwa H, et al. Surgical strategy for cervical dumbbell tumors based on a three-dimensional classification. *Spine (Phila Pa 1976)* 2004;29:E10-4.
- Pucci JU, Christophe BR, Sisti JA, et al. Three-dimensional printing: technologies, applications, and limitations in neurosurgery. *Biotechnol Adv* 2017;35:521-9.
- He S, Yang X, Yang J, et al. Customized “whole-cervical-vertebral-body” reconstruction after modified subtotal spondylectomy of C2-C7 spinal tumor via piezoelectric surgery. *Oper Neurosurg (Hagerstown)* 2019;17:580-7.
- Xu N, Wei F, Liu X, et al. Reconstruction of the upper cervical spine using a personalized 3D-printed vertebral body in an adolescent with ewing sarcoma. *Spine (Phila Pa 1976)* 2016;41:E50-4.
- Li X, Wang Y, Zhao Y, et al. Multilevel 3D printing implant for reconstructing cervical spine with metastatic papillary thyroid carcinoma. *Spine (Phila Pa 1976)* 2017;42:E1326-30.
- Choy WJ, Mobbs RJ, Wilcox B, et al. Reconstruction of thoracic spine using a personalized 3D-printed vertebral body in adolescent with T9 primary bone tumor. *World Neurosurg* 2017;105:1032.e13-7.
- Yang J, Cai H, Lv J, et al. In vivo study of a self-stabilizing artificial vertebral body fabricated by electron beam melting. *Spine (Phila Pa 1976)* 2014;39:E486-92.
- Yang J, Cai H, Lv J, et al. Biomechanical and histological evaluation of roughened surface titanium screws fabricated by electron beam melting. *PLoS One* 2014;9:e96179.
- Jian Q, Xu WL, Duan WR, et al. Clinical observation on the application of customized 3D printed prosthetic body weight in the treatment of axial tumors. *Chin J Spine Spinal Cord* 2020;30:804-10.
- Enneking WF, Spanier SS, Goodman MA. A system for the surgical staging of musculoskeletal sarcoma. *Clin Orthop Relat Res* 1980;(153):106-20.
- Hart RA, Boriani S, Biagini R, et al. A system for surgical staging and management of spine tumors. A clinical outcome study of giant cell tumors of the spine. *Spine (Phila Pa 1976)* 1997;22:1773-82.
- Ozawa H, Kokubun S, Aizawa T, et al. Spinal dumbbell tumors: an analysis of a series of 118 cases. *J Neurosurg Spine* 2007;7:587-93.
- Raynor RB, Moskovich R, Zidel P, et al. Alterations in primary and coupled neck motions after facetectomy. *Neurosurgery* 1987;21:681-7.
- Bongioanni F, Assadurian E, Polivka M, et al. Aneurysmal bone cyst of the atlas: operative removal through an anterolateral approach. A case report. *J Bone Joint Surg Am* 1996;78:1574-7.
- Suchomel P, Buchvald P, Barsa P, et al. Single-stage total C-2 intralesional spondylectomy for chordoma with three-column reconstruction. Technical note. *J Neurosurg Spine* 2007;6:611-8.
- Wang VY, Deviren V, Ames CP. Reconstruction of C-1 lateral mass with titanium mesh cage after resection of an aneurysmal bone cyst of the atlas. *J Neurosurg Spine* 2009;10:117-21.
- Chung JY, Kim JD, Park GH, et al. Occipitocervical reconstruction through direct lateral and posterior approach for the treatment of primary osteosarcoma in the atlas: a case report. *Spine (Phila Pa 1976)* 2012;37:E126-32.
- Jandial R, Kelly B, Bucklen B, et al. Axial spondylectomy and circumferential reconstruction via a posterior approach. *Neurosurgery* 2013;72:300-8.
- Winking M. Lateral mass lesions of the C1 vertebra: a modified “far lateral” approach. *Eur Spine J* 2014;23 Suppl 2:257-61.
- Bobinski L, Levivier M, Duff JM. Occipitoaxial spinal interarticular stabilization with vertebral artery preservation for atlantal lateral mass failure. *J Neurosurg Spine* 2015;22:134-8.
- Clarke MJ, Zadnik PL, Groves ML, et al. Fusion following lateral mass reconstruction in the cervical spine. *J Neurosurg Spine* 2015;22:139-50.
- Clarke MJ, Price DL, Cloft HJ, et al. En bloc resection of a C-1 lateral mass osteosarcoma: technical note. *J Neurosurg Pediatr* 2016;18:46-52.
- Peciu-Florianu I, Chittur Viswanathan G, Barges-Coll J, et al. Bilateral C-1 lateral mass reconstruction following radical resection of a giant osteoblastoma of the atlas: case report. *J Neurosurg Spine* 2017;26:307-12.
- Stephens BH, Wright NM. Reconstruction of the C-1 lateral mass with a titanium expandable cage after resection of eosinophilic granuloma in an adult patient. *J Neurosurg Spine* 2017;26:252-6.

27. Neva J, Smith BW, Joseph JR, et al. Use of intraoperative navigation for reconstruction of the C1 lateral mass after resection of aneurysmal bone cyst. *World Neurosurg* 2017;102:693.e21-7.
28. Ji W, Cheng Y, Zhu Q, et al. Posterior unilateral exposure and stability reconstruction with pedicle and lamina screw fixation for the cervical dumbbell tumorectomy: a case report and biomechanical study. *Eur Spine J* 2021;30:568-75.
29. Eleraky M, Setzer M, Vrionis FD. Posterior transpedicular corpectomy for malignant cervical spine tumors. *Eur Spine J* 2010;19:257-62.
30. Yang X, Wu Z, Xiao J, et al. Sequentially staged resection and 2-column reconstruction for C2 tumors through a combined anterior retropharyngeal-posterior approach: surgical technique and results in 11 patients. *Neurosurgery* 2011;69(2 Suppl Operative):ons184-93; discussion ons193-4.
31. Jeszenszky D, Fekete TF, Melcher R, et al. C2 prosthesis: anterior upper cervical fixation device to reconstruct the second cervical vertebra. *Eur Spine J* 2007;16:1695-700.
32. Stulík J, Kozák J, Sebesta P, et al. Total spondylectomy of C2: a new surgical technique. *Acta Chir Orthop Traumatol Cech* 2007;74:79-90.
33. Ames CP, Wang VY, Deviren V, et al. Posterior transpedicular corpectomy and reconstruction of the axial vertebra for metastatic tumor. *J Neurosurg Spine* 2009;10:111-6.
34. Hunn SAM, Koefman AJ, Hunn AWM. 3D-printed titanium prosthetic reconstruction of the C2 vertebra: techniques and outcomes of three consecutive cases. *Spine (Phila Pa 1976)* 2020;45:667-72.
35. Pal GP, Sherk HH. The vertical stability of the cervical spine. *Spine (Phila Pa 1976)* 1988;13:447-9.
36. Dorweiler B, Baqué PE, Chaban R, et al. Quality control in 3D printing: accuracy analysis of 3D-printed models of patient-specific anatomy. *Materials (Basel)* 2021;14:1021.
37. Martelli N, Serrano C, van den Brink H, et al. Advantages and disadvantages of 3-dimensional printing in surgery: a systematic review. *Surgery* 2016;159:1485-500.
38. McGilvray KC, Easley J, Seim HB, et al. Bony ingrowth potential of 3D-printed porous titanium alloy: a direct comparison of interbody cage materials in an in vivo ovine lumbar fusion model. *Spine J* 2018;18:1250-60.